Optics Letters

Topology-optimized metasurfaces: impact of initial geometric layout

JIANJI YANG AND JONATHAN A. FAN*

Department of Electrical Engineering, Stanford University, Stanford, California 94305, USA
**Corresponding author: jonfan@stanford.edu*

Received 27 June 2017; revised 19 July 2017; accepted 19 July 2017; posted 20 July 2017 (Doc. ID 298102); published 9 August 2017

Topology optimization is a powerful iterative inverse design technique in metasurface engineering and can transform an initial layout into a high-performance device. With this method, devices are optimized within a local design phase space, making the identification of suitable initial geometries essential. In this Letter, we examine the impact of initial geometric layout on the performance of large-angle (75 deg) topology-optimized metagrating deflectors. We find that when conventional metasurface designs based on dielectric nanoposts are used as initial layouts for topology optimization, the final devices have efficiencies around 65%. In contrast, when random initial layouts are used, the final devices have ultra-high efficiencies that can reach 94%. Our numerical experiments suggest that device topologies based on conventional metasurface designs may not be suitable to produce ultra-high-efficiency, large-angle metasurfaces. Rather, initial geometric layouts with non-trivial topologies and shapes are required.

OCIS codes: (230.1950) Diffraction gratings; (160.3918) Metamaterials; (310.6628) Subwavelength structures, nanostructures; (310.6805) Theory and design; (350.4238) Nanophotonics and photonic crystals; (230.1360) Beam splitters.

https://doi.org/10.1364/OL.42.003161

Metasurfaces [1] are nanostructured thin films that can support effective wavefront shaping with nanoscopic footprints, potentially enabling ultra-compact optical systems. To date, transmissive metasurfaces made from lossless dielectric materials have been implemented as gratings [2–4], lenses [5–7], holograms [8], wavelength splitters [4,9], and polarization-sensitive phase plates [10,11]. Significant efforts have been made to expand the scope of these devices to incorporate large bending angles [3,12,13], an essential feature for a broad range of applications. For microscopy, large numerical aperture lenses, which support high spatial resolution imaging and large light collection efficiencies, require large bending angles. In display technologies, wide field-of-view observation requires light to be bent to a large range of solid angles. For many practical applications in beam steering, large-angle beam deflection is required.

In conventional metasurface designs, subwavelength-scale elements with discrete phase responses, such as nanowaveguides or nanoresonators, are stitched together to produce a desired phase profile response [1,6]. With these schemes, devices have relatively high efficiencies for low to moderate bending angles. [2,4]. However, for bending angles larger than 50 deg, the efficiencies drop considerably [4]. An alternative design strategy is based on adjoint-based topology optimization, which is an iterative optimization procedure that can produce high-performance metasurface devices composed of non-intuitive, curvilinear patterns [4,14]. In this inverse design approach, a spatial distribution of dielectric material, which serves as the initial geometry for the design, is transformed to a final binary layout (e.g., silicon nanostructures in air [4]) over multiple iterations. The desired function of the device is cast as a figure of merit and, during each iteration, the dielectric material is modified in a manner that improves the figure of merit. Compared to other heuristic design schemes, such as those based on genetic and thermal annealing algorithms, topology optimization presents significant advantages in computational efficiency. This design method has been used by our group to experimentally produce silicon-based periodic metasurfaces (i.e., metagratings) that deflect light to bending angles as large as 75 deg with high efficiencies [4]. It has also been used to theoretically construct ultra-high efficiency metasurfaces consisting of multiple layers of silicon-silicon dioxide nanostructures, such as ultra-large angle deflectors (>85 deg), spectral filters, and angular-selective filters [15]. The exceptional performance from all of these topology-optimized devices originates from light-matter interactions based on intricate mode coupling and scattering dynamics [14].

Mathematically, topology optimization is based on the method of gradient descent, in which initial geometries are *iteratively* optimized within *local* design phase spaces (subsets of global phase space) to produce the final devices (local optima) [16]. As such, the potential for this design strategy to yield exceptional devices is predicated on the identification of initial geometries located within suitable local design phase spaces. Unfortunately, there currently exist no effective, predictable methods for specifying good initial geometries for topology optimization. In prior work with large-angle metagratings [4,14], random spatial distributions of dielectric material were used as initial geometries, and a subset of these structures produced devices with exceptional efficiencies. An open question is

whether simple discrete shapes, such as those used in conventional metasurface designs [1,5,10,11], could serve as good initial geometries. If so, a systematic design method that combines conventional metasurface engineering with topology optimization could serve as a general and scalable route towards high-performance, large-area metasurfaces.

In this Letter, we explore the use of initial geometries based on simple discrete shapes [2,10] for transmissive, topology-optimized metagrating devices. As a model system, we study metagratings that deflect unpolarized incident plane waves with a wavelength $\lambda_0 = 1050$ nm to 75 deg (+1 diffraction order), shown in Fig. 1(a). We consider initial geometries consisting of 800 nm tall silicon nanoposts per metagrating supercell, which mimic the geometries of conventional dielectric metasurface designs [2,10]. We find that when topology optimization is applied to initial geometries made of silicon nanoposts, the efficiencies of the resulting devices are boosted from 0%–30% to the 60%–80% range. However, these efficiencies are still significantly lower than those of devices optimized using random starting point structures, which can have efficiencies exceeding 90% [4,14]. These results indicate that the local design phase spaces specified by nanopost-based initial geometries may not support exceptionally high efficiencies. Rather, ultra-high-efficiency devices require more topologically complex starting point structures, which can be captured with random structures consisting of a continuous distribution of dielectric constants.

We begin our analysis by evaluating the performance of metagratings containing cylindrical nanoposts, which will then be used as initial geometries in our topology optimization algorithm. Following the conventional metasurface approach [2,10], we consider only two nanoposts per metagrating supercell to minimize near-field optical coupling between posts. The magnitude and phase response of these silicon nanoposts are determined through full-wave simulations [17] of subwavelength gratings with a period equal to $\lambda_0/2$ [2,10]. From these simulations, we find that posts with diameters ranging from 80 to 260 nm can cover phase responses ranging from 0 to 2π and support light transmission above 90%. Our choice of post geometry parameters, including thicknesses, diameters, and center-to-center separations, is consistent with those in other nanopost-based metasurfaces [2,10,11].

We first consider metagratings with posts that are separated by a fixed distance equal to half the supercell period along the x-axis. This design approach follows from conventional approaches for blazed metagrating design, in which nanoposts of varying diameters serve as phase-delay components that sample the 0–2π linear phase profile over a metagrating supercell. To ensure that layouts with optimal post diameters are identified, we sweep the diameters of each post in the metagrating from 80 to 260 nm and compute the resulting device efficiencies. The results are plotted in Fig. 1(b) and show that most combinations of nanopost diameters do not effectively deflect light to a 75 deg angle. However, there are a few devices that support modest efficiencies in the 30% range, and the best device has a deflection efficiency of 37%. These efficiency levels are consistent with those of benchmark calculations previously performed for conventional metasurface designs [4].

To further expand the design space for two-nanopost systems, we identified the optimal distances between posts for each combination of post diameters in the metagrating, using brute-force parameter sweeping. The results are summarized in Fig. 1(c) and show that the general efficiency trends in the contour plot are qualitatively similar to those of nanoposts with fixed spacing in Fig. 1(b). These similarities indicate that the optimization of separation distance between nanoposts leads to relatively modest and local changes within the design phase space. Select devices support efficiencies in the 40%–50% range. Compared to the devices in Fig. 1(b), these efficiencies are improved, but are still relatively low.

We use the nanopost-based designs in Fig. 1(c) as initial geometries for our topology optimization algorithms [4] to understand how conventional metasurface designs can be used in inverse design. The results are summarized in Fig. 1(d) and show that for all combinations of post diameters, all the topology-optimized devices have efficiencies above 55%. Even initial geometries that possess nearly 0% deflection efficiency evolve to devices with much higher efficiencies. The best device has a deflection efficiency of 78%, marked by the gray box in Fig. 1(d). These results indicate that topology optimization is capable of searching through a broad design phase space to identify high-efficiency devices.

Surprisingly, the best topology-optimized device has an initial geometry, marked by the red box in Fig. 1(c), which possesses an efficiency of only 8%. This observation indicates that while relatively simple shapes can be used as a good starting

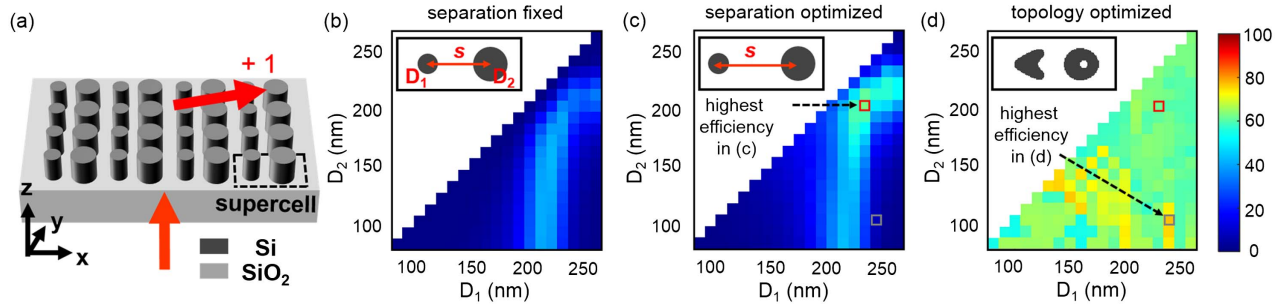

Fig. 1. Efficiency calculations for 75 deg metagratings. (a) Schematic of a metagrating with two silicon nanoposts per grating supercell. (b) Efficiencies of metagratings made of two silicon nanoposts per metagrating supercell. The center-to-center separations (s) of the posts are fixed to be half the metagrating supercell period along the x-axis. The diameters of the two nanoposts are D1 and D2. (c) Efficiency of two-nanopost metagratings with optimal s. For each (D_1, D_2) combination, the optimal separation is determined by sweeping s. (d) Efficiency of metagratings optimized by a topology optimization approach. The initial geometries used in topology optimization are the nanopost-based metagratings in (c). For all the metagratings under study here, the supercell size is $[\lambda_0/\sin(0.417\pi), \lambda_0/2]$, the device thickness is 800 nm, and the operation wavelength is $\lambda_0 = 1050$ nm. The insets in (b)–(d) show the top-view layouts of the supercells.

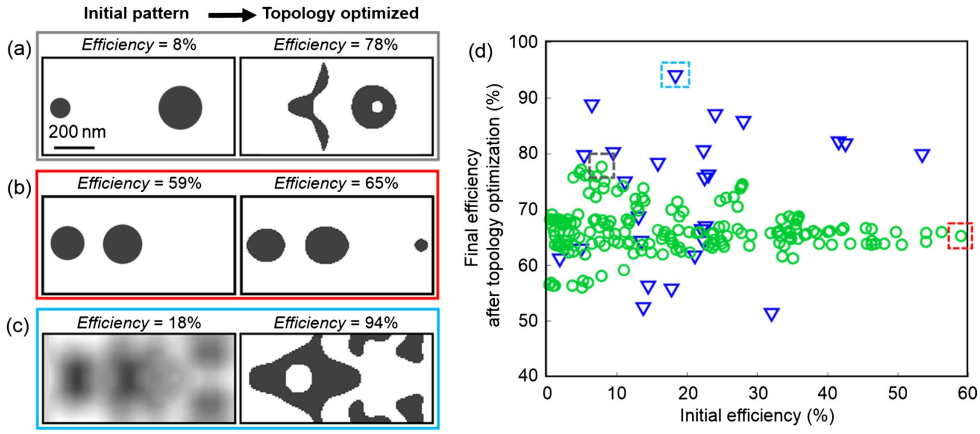

Fig. 2. Initial geometries and final layouts of topology-optimized metagratings in a supercell. (a) Layout of the initial device (left) that produces the highest-efficiency topology-optimized metagrating (right) for nanopost-based initial geometries. (b) Layout of the post-based device with the highest initial efficiency (left) and its design after topology optimization. (c) Layout of a random initial pattern (left) and the resulting high-efficiency freeform metagrating generated by topology optimization. (d) Realizations obtained using topology optimization, with nanopost-based metagratings (green circles, 190 in total) and random material distribution (blue triangles, 26 in total) as initial patterns. The outline coloring in (a) and (b) correspond to markings in Figs. 1(c) and 1(d) and to the boxes in (d); the outline coloring in (c) corresponds to the marking in (d). Visualization 1, Visualization 2, and Visualization 3 showing the iterative topology optimization process for (a)–(c) are in the Supplementary Materials.

design, the detailed geometric specifications of these good shapes may not correspond with the highest-efficiency structures based on conventional metagrating designs. The layouts of this device before and after optimization are presented in Fig. 2(a) and show that the initial geometry and final device are topologically similar, with each containing two dielectric structures.

However, the post-based geometry with the best initial efficiency [red box in Fig. 1(c)] evolves to a topology-optimized device with an efficiency of only 65% [red box in Fig. 1(d)]. This value is significantly lower than that produced by the best topology-optimized device in Fig. 1(d), and it is among the lower values in this plot. The layouts of this device before and after optimization are presented in Fig. 2(b) and appear to be qualitatively similar. This initial geometry, which represents an optimal conventional metasurface design, resides in a limited local design phase space that restricts substantial efficiency improvements with topology optimization.

While devices optimized from nanopost-based initial geometries can support high efficiencies, they are strongly outperformed by devices optimized from random initial geometries, which can operate with over 90% efficiency. Unlike nanopost-based structures, random structures contain nontrivial topological features that span the entire grating unit cell. As such, designs evolved from these initial geometries contain complex, curvilinear features spanning the unit cell [Fig. 2(c)]. The origins of ultra-high-efficiency beam deflection in these freeform metagratings can be attributed to intricate optical mode dynamics. In a prior study, we showed that the optical modes in high-performance metagratings undergo intra-mode and inter-mode coupling at the metagrating-substrate and metagrating-air interfaces, which lead to complex multiple scattering behavior [14].

To summarize and benchmark the different metasurface design approaches studied here, we plot in Fig. 2(d) a distribution of final metagrating efficiencies, as obtained from different types of initial geometries. The highest efficiencies are achieved in devices designed using random initial geometries (blue triangles), which are then evolved by topology optimization, and have efficiencies as high as 94%. We note that upon optimizing an ensemble of different initial geometries, only a fraction of final devices exhibit ultra-high efficiencies. As such, multiple optimization attempts are required to identify devices with exceptional efficiencies.

The efficiencies of devices designed from post-based initial geometries, followed by topology optimization, are also plotted in Fig. 2(d) and generally cluster in the 55%–80% range (green circles). Of these devices, those exhibiting relatively high final efficiencies have initial geometries that possess relatively low efficiencies. This indicates that simple shapes may be used as initial geometries in topology optimization to produce high-efficiency designs, but the detailed geometric configuration of these shapes may not correspond to conventional metagrating designs. The highest-efficiency post-based devices that are not refined with topology optimization [Fig. 1(c)] possess efficiencies below 50% and perform worse than all of the topology-optimized metagratings in Fig. 2(d), signifying the limitations of large-angle metagratings based exclusively on simple cylindrical post structures.

In summary, we have shown that topology optimization is a powerful design tool for realizing high-efficiency large-angle metasurface deflectors. Topology-optimized devices that use conventional post-based metasurface designs as initial geometries exhibit limited performance, indicating that conventional metasurfaces do not possess geometric topologies suitable for ultra-high-performance, large-angle deflection. On the other hand, devices optimized using random initial geometries can possess exceptionally high efficiencies of over 90%. A current limitation of this random geometry approach is that multiple random geometries may be required to be optimized before a high-performance device is identified, which is computationally demanding. Innovations in the systematic identification of proper initial geometries will be necessary to enable the efficient implementation of topology optimization in large-area

metasurfaces. We envision that our analysis will apply to and facilitate the development of high-performance aperiodic metasurfaces, as well as other classes of integrated photonic optical components [18,19].

Funding. Office of Naval Research (ONR) (N00014-16-1-2630); Packard Fellowship Foundation.

Acknowledgment. Part of the simulations were performed in the Sherlock computing cluster at Stanford University. The authors thank Sage Doshay for the critical reading of the manuscript.

REFERENCES

1. N. Yu and F. Capasso, Nat. Mater. **13**, 139 (2014).
2. P. Lalanne, S. Astilean, P. Chavel, E. Cambril, and H. Launois, Opt. Lett. **23**, 1081 (1998).
3. D. Sell, J. Yang, S. Doshay, K. Zhang, and J. A. Fan, ACS Photon. **3**, 1919 (2016).
4. D. Sell, J. Yang, S. Doshay, R. Yang, and J. A. Fan, Nano Lett. **17**, 3752 (2017).
5. M. Khorasaninejad, W. T. Chen, R. C. Devlin, J. Oh, A. Y. Zhu, and F. Capasso, Science **352**, 1190 (2016).
6. D. Lin, P. Fan, E. Hasman, and M. L. Brongersma, Science **345**, 298 (2014).
7. P. Lalanne, S. Astilean, P. Chavel, E. Cambril, and H. Launois, J. Opt. Soc. Am. A **16**, 1143 (1999).
8. L. Wang, S. Kruk, H. Tang, T. Li, I. Kravchenko, D. N. Neshev, and Y. S. Kivshar, Optica **3**, 1504 (2016).
9. D. Sell, J. Yang, S. Doshay, and J. A. Fan (2017) (submitted).
10. A. Arbabi, Y. Horie, M. Bagheri, and A. Faraon, Nat. Nanotechnol. **10**, 937 (2015).
11. M. P. Backlund, A. Arbabi, P. N. Petrov, E. Arbabi, S. Saurabh, A. Faraon, and W. E. Moerner, Nat. Photonics **10**, 459 (2016).
12. V. S. Asadchy, A. Wickberg, A. Díaz-Rubio, and M. Wegener, ACS Photon. **4**, 1264 (2017).
13. N. M. Estakhri and A. Alù, Phys. Rev. X **6**, 041008 (2016).
14. J. Yang, D. Sell, and J. A. Fan (2017) (submitted).
15. J. A. Fan, D. Sell, and J. Yang, "Device components formed of multiple layers of geometric structures or a three dimensional multi-layer, multi-material metasurface," U.S. provisional patent 62/329,841 (2016).
16. M. P. Bendsoe and O. Sigmund, *Topology Optimization: Theory, Methods, and Applications* (Springer, 2003).
17. J. P. Hugonin and P. Lalanne, *Reticolo Software for Grating Analysis* (Institut d'Optique, 2005).
18. J. Lu and J. Vučković, Opt. Express **21**, 13351 (2013).
19. L. F. Frellsen, Y. Ding, O. Sigmund, and L. H. Frandsen, Opt. Express **24**, 16866 (2016).